# Direct Numerical Simulation of Jet Actuators for Boundary Layer Control

Björn Selent and Ulrich Rist

Universität Stuttgart, Institut für Aero- & Gasdynamik, Pfaffenwaldring 21, 70569 Stuttgart, Germany,
`selent@iag.uni-stuttgart.de`, `rist@iag.uni-stuttgart.de`,
WWW home page: `http://www.iag.uni-stuttgart.de`

## Summary

The paper presents a method to perform direct numerical simulations (DNS) of a jet actuator flow inside a turbulent flat plate boundary layer (TBL). A structured finite difference method is used for the simulations. The numerical scheme is adapted to account for the large scale differences both in geometric and fluid dynamic aspect. Analytical mesh transformations have been implemented to resolve the jet orifice. Suitable boundary conditions are established to model the jet flow. Numerical stability has been added by implementing a compact filter scheme. The TBL baseflow is generated by mimicing experimental approaches and direct simulation of the laminar-turbulent transition process. Simulations of a jet actuator configuration perturbing the turbulent baseflow have been undertaken and the results are evaluated.

## 1 Introduction

Jet actuators or jet vortex generators (JVG) have been proven to provide a mechanism to positively control boundary layer flows. Experimental work by Johnston et. al. [1] has shown the general ability to suppress separation in flows with adverse pressure gradient. The effect stems from the fact that longitudinal vortices are established inside the boundary layer and a mixing of the BL's faster layers with low-speed layers closer to the wall takes place. The mixing in turn leads to increased skin friction thus enabling the flow to overcome larger pressure gradients downstream. This is a very similar effect observed from passive vortex generators [2]. The advantage of jet vortex generator systems over existing solid generators lies in their flexibility to be applied only when necessary and thus to avoid any parasitic drag. An exhaustive parameter study was undertaken by Godard et. al. [3] covering many aspects of jet actuators such as velocity ratio $\lambda$, skew angle $\beta$ and pitch angle $\alpha$, hole geometry and direction of rotation. The tested configurations were compared by the increase of skin friction induced by the vortex. From these values the authors deduced an optimum jet configuration. Recent publications also report on the interaction of vortices generated by staggered actuator arrays [4]. For evaluation a momentum integral was used in this case and it was documented that jet arrays

were capable of prolonging the positive effect of the vortices further downstream compared to a single line of actuators.

Albeit the outcomes of these experiments yield a very good general idea of the mechanism of active flow control devices there still are a number of open questions involved as no detailed picture of the forming of the vortex and its interaction with the boundary layer could be gained from experiment yet. Therefore, any design suggestions for actuators rely heavily on empirical data and are difficult to transpose to different configurations. Within the AERONEXT research program numerical simulations of jet actuators are to be performed by means of RANS and DNS technique. The regime considered consists of a strong steady jet disturbance in a flat-plate turbulent boundary layer cross flow. Since RANS simulations allow for a faster computation they are well suited to cover numerical parameter studies. The DNS approach on the other hand was chosen for its lack of any model assumptions. Therefore, it is well suited to provide a reference solution for coarser numerical schemes. Furthermore, DNS allows for a computation of the unsteady flow formation especially in the beginning of the vortex generation and detailed analysis of the fluid dynamics involved.

## 2 Numerical Method

All simulations have been performed using the program *NS3D*, developed at IAG. The method utilizes a hybrid finite difference/spectral scheme for spatial discretization and a standard explicit Runge-Kutte method for time integration. The program is both shared and distributed memory parallelized using MPI and NEC Microtasking programming techniques. Additionally the structured mesh approach allows for strong vectorization on the NEC SX8 platform used.

The program *NS3D* solves the compressible unsteady conservation equations in conservative form on a three dimensional Cartesian mesh. Spatial derivatives in downstream and wall-normal direction are approximated by compact finite differences of order $(O6)$ with spectral like resolution [5]. Derivatives on the domain boundaries are approximated by one sided finite differences of order $(O4)$. Reduction of order on the boundaries takes place in order to avoid strong numerical damping due to the one-sided stencil. In spanwise direction periodicity is assumed and a spectral method is used to compute spatial derivatives.

Time integration is performed by a standard four-step Runge-Kutta scheme of order $(O4)$. In between the RK sub steps as well as in between full time steps the FD stencils are shifted forward and backward alternately thus introducing numerical dissipation and generating a more robust scheme [6].

At the inflow subsonic characteristic boundary conditions are used. At the free-stream boundary exponential decay of all disturbances in wall-normal direction is prescribed. At the outflow boundary a relaminarization zone is applied. The wall is assumed to be isothermal and no-slip boundary conditions are used, the wall-normal pressure gradient is assumed to equal zero. Periodic boundary conditions are applied in spanwise direction. Fluctuations are introduced via inhomogeneous

wall boundary conditions. In this manner wave like periodic disturbances as well as continuous or cyclic suction and blowing can be realized on the wall.

Initial conditions describe laminar flow on a flat plate with zero pressure gradient.

# 3  Jet Vortex Generator Simulations

The very nature of jet vortex generator flow simulations poses a number of challenges which need to be addressed.

Firstly, the physical domain size and resolution are determined by the actuator exit geometry and jet dimensions respectively and the downstream development of the induced vortex itself. The resulting scale differences are in the order of magnitude of $L/d = 10^2$. Therefore suitable analytical mesh transformations have been implemented to assure sufficient resolution on both ends of the scale. These transformations allow for mesh compression over the jet orifice and a stretching of the mesh towards the domain boundaries. The actuator is not modelled but the emerging jet is introduced through inhomogeneous boundary conditions. A polynomial of order $(O5)$ is used to prescribe the velocity distribution at the jet exit. The implementation also allows for an arbitrary skew and pitch of the jet.

Secondly, the computational scheme is based on the compressible form of the Navier-Stokes equations. The scheme was chosen in order to be able to model the speed range that is encountered for commercial aircraft. Experimental results agree on the need for a large jet-to-freestream-velocity ratio $\lambda \approx 5$ for efficient vortex generation. In order to avoid transonic effects, the free stream Mach number thus needs to be quite small ($Ma \approx 0.15 - 0.2$). For small $Ma$ the formulation exhibits increasingly singular behaviour which has to be accounted for by decreasing the time step to a level at which dissipation due to forward-backward shifting no longer suffices for stable computations. Thus, a compact filter was implemented to stabilize the computations [5].

## 3.1  Turbulent Boundary Layer

In order to obtain a turbulent baseflow an approach is chosen which mimics experimental setups. Wavelike disturbances are introduced into a laminar boundary layer and the laminar-turbulent transition is simulated. Suchlike any assumptions of eddy size and frequencies contained in the turbulent spectrum are avoided. The goal is to generate a TBL satisfying the statistical properties of turbulence for a designated Reynolds number based on momentum thickness $Re_\Theta$. It was found that breakdown could be reached fastest using a 2D Tollmien-Schlichting (TS) and a subharmonic 3D wave in combination with a steady homogenous 2D disturbance. The steady disturbance inflicts an inflection point into the laminar profile. A good picture of the effectivity of the tripwire/subharmonic scenario can be gained from figure 1(a). Shown are the maximum amplitudes of the fundamental frequency obtained from FFT analysis of the downstream velocity $u' = u_{turb} - U_0$ with turbulent velocity

field $u_{turb}$ and steady laminar velocity field $U_0$. The graph can be read as description of the baseflow change due to the perturbations. The fully turbulent state is reached farther upstream for the tripwire/subharmonic breakdown compared to the purely subharmonic case. Figure 1(b) depicts a comparison of the displacement and momentum thickness of the boundary layer. The shape factor $H_{12} = \delta_1/\theta$ converges to 1.3 in both cases but at smaller $Re_x$ values for the tripwire case.



(a) Maximum amplitudes of baseflow change

(b) BL thickness, shape factor
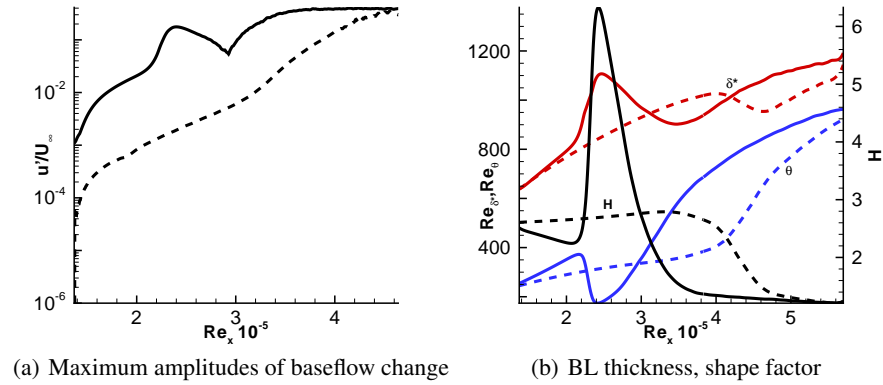
**Figure 1**   Comparison of transition scenarios, solid lines: tripwire, dashed lines: purely subharmonic

The tripwire/subharmonic perturbations have been used to generate a turbulent reference flow of a boundary layer on a flat plate with zero pressure gradient. The physical parameters for the computation are as follows: $Re = 100000$, based on freestream velocity $U_\infty = 52m/s$, kinematic viscosity $\nu = 1.5 \cdot 10^{-5} m^2/s$ and characteristic length $L = 30mm$. The mesh consists of 1200x300x128 nodes in $x$, $y$ and $z$ directions. Mesh spacings in wall units based on $u_\tau = \sqrt{\frac{\tau}{\rho}}$ are $\Delta x^+ \approx 12$, $\Delta y^+ \approx 1$, $\Delta z^+ \approx 6$ and the time step is $\Delta t = 3.9 \cdot 10^{-5}$. The turbulent flow at $Re_\theta = 800$ is compared quantitatively with both numerical and experimental data and the results are shown in figure 2. The turbulent velocity profile is in very good agreement with data taken from Spalart [7] and TU Braunschweig (fig. 2(a)). The rms fluctuations of the spanwise velocity in wall units (fig. 2(b)) is in good agreement with data from Spalart's numerical simulations. Deviations to Spalart's values in downstream and wall-normal direction originate most likely from the compact difference formulation and might be reduced by decreasing $\Delta x$ and $\Delta y$. Within the context of a JVG simulation the TBL deems sufficiently resolved nonetheless and was used as baseflow for following computations.

(a) Turbulent mean velocity profile      (b) RMS values of velocity based on $u_\tau$
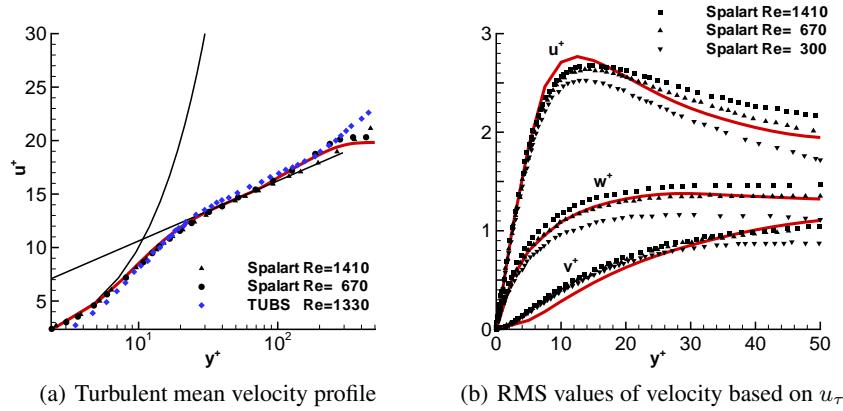
**Figure 2**    Turbulent BL, red lines: present computation at $Re_\Theta = 800$

## 3.2   Jet Vortex Generator in TBL

Into the TBL baseflow a Jet Vortex Generator was included in subsequent simulations. The jet-to-freestream velocity ratio is $\lambda = 5.2$ and jet exit radius $r = 1mm$. The jet is pitched by $\alpha = 30°$ and skewed to the freestream by $\beta = 80°$. Nozzle distance is set to $2D$ in spanwise direction. The jet centre is positioned at $x = 4.3$. Figure 3 depicts isosurfaces of the vortex identification criterion $\lambda_2$ [8] after 144 hrs of computation. It can be seen how a crossflow jet is formed downstream of the nozzle. The jet develops ring-like vortices along its trajectory which interfere with each other. The jet is highly unstable and almost complete breakdown of distinct jet structures takes place over a short distance downstream. A region of increased vorticity develops behind the jet. Figure 4 depicts time averaged velocity contours of the downstream velocity and velocity vectors in the transverse plane. Shown are four stations in order to obtain an insight in the evolution of the flow due to the jet. The first station at $x = 3.8$ is situated upstream of the jet. It can be seen how the flow already exhibits a wavy structure because of the blockage of the boundary layer before the jets. At $x = 4.4$ a rotational motion can be observed which mixes the layers inside the boundary layer. Low-speed fluid is entrained upwards. On the top outward side of these vortices a high-speed streak is established. Farther downstream at $x = 4.8$ alternating low- and high-speed streak structures are present and the vector field shows a strong spanwise motion. At this station only a small rotational motion is measured. At the last position $x = 5.2$ the flow does not contain distinct structures anymore. The streaks and vortices have almost completely dissipated. For the purpose of separation control, the increase of wall friction is of interest. Figure 5(a) depicts the spanwise mean and time averaged change of wall friction coefficient of the perturbed flow based on the corresponding value for the undisturbed flow over $x$. In a close distance downstream of the nozzle a negative effect can be
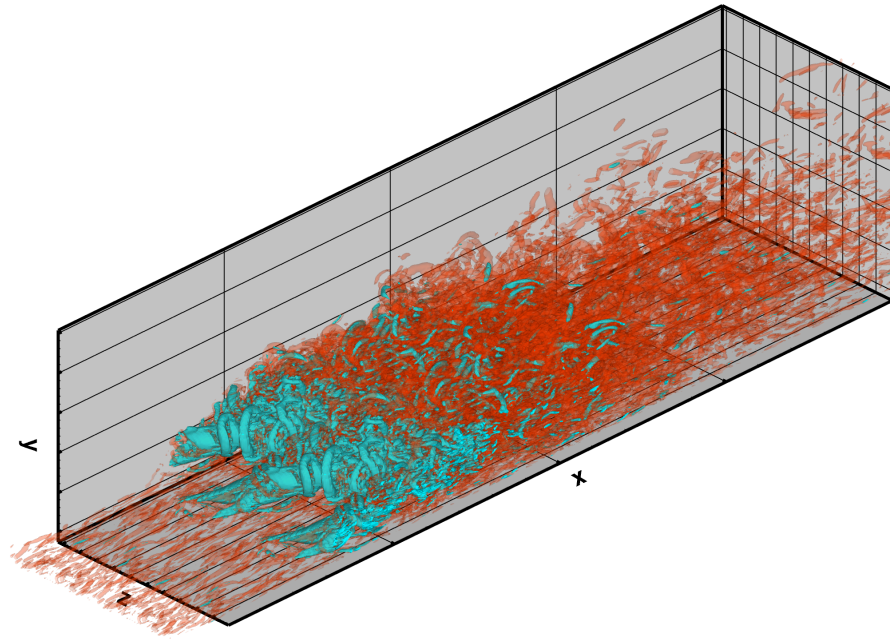
**Figure 3**    Jet in TBL, Ma=0.15, $\lambda = 5.2$, blue: isosurface $\lambda_2 = -2000$, red: isosurface $\lambda_2 = -200$
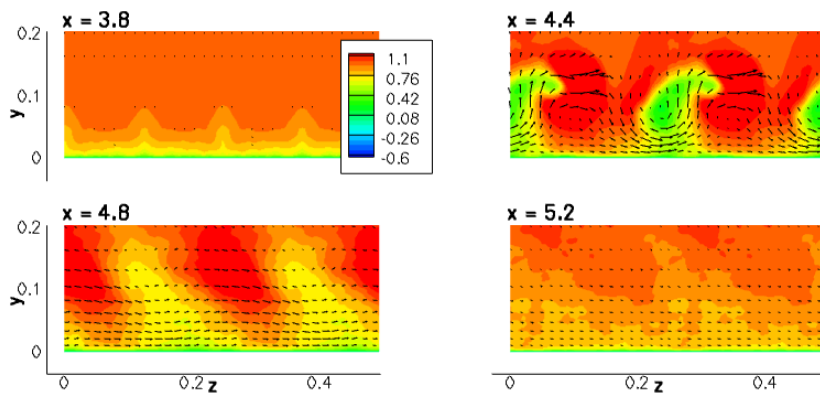


**Figure 4**    Vortex and streak development caused by JVG, contours represent mean $u$ velocity. Arrows are velocity vectors in $y$-$z$-plane
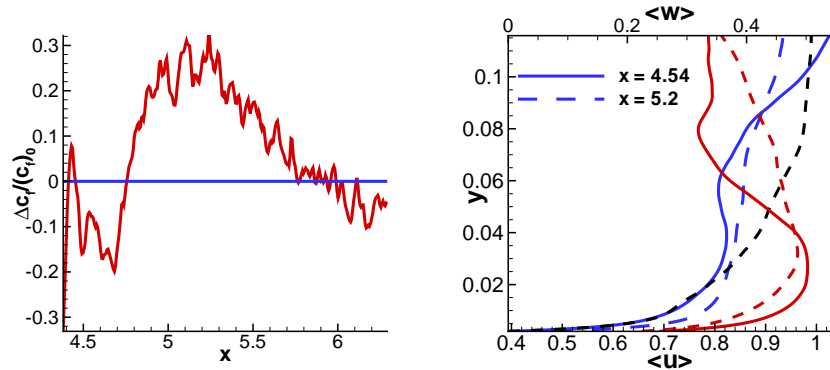
(a) Change of wall friction coefficient, blue line indicates no change.

(b) Time averaged mean spanwise velocity, blue line: $u$, red line: $w$, black line: $u$ of reference

**Figure 5**  Effect of JVG in TBL

seen. The wall friction decreases compared to the baseflow. This is because the jet imposes entrainment on the boundary layer whereas the induced rotational motion is not strong enough to feed high-speed fluid in the near wall regions. Downstream of $x = 4.8$ a region of increased wall friction is visible which corresponds to the streak area described in figure 4. Here the additional momentum of the jet is directed into a crossflow motion. Representative spanwise mean and time averaged velocities are plotted in figure 5(b). Compared to the reference TBL flow the $u$ veloctiy at $x = 4.54$ does not show an increase close to the wall but a strong velocity defect in the overlap region. The $u$ velocity at station $x = 5.2$ on the other hand indicates a transfer of momentum towards the wall whereas the defect in the overlap is diminished. The spanwise velocity at $x = 4.54$ contains strong gradients which might result from taking the mean over regions with alternating strong and weak spanwise motion as seen in figure 4 at $x = 4.4$. Farther downstream the $w$ profile is more uniform which indicates a directed crossflow over the whole span. The maximum value for $w$ is decreasing while travelling downstream due to dissipation. The positive effect of increased friction is lost after a short distance downstream of about $\Delta x = 25D$. The simulated configuration suffers somewhat from the close spanwise distance of the nozzles. Therefore, the anticipated effect of generating a longitudinal vortex in the flow is not reached. The momentum input of the jet is mostly used to deflect the flow in spanwise direction rather than to increase the momentum close to the wall in downstream direction.

# 4 Conclusions

A numerical scheme is presented for direct numerical simulations of jet vortex generators in turbulent boundary layers. The method is based on the fully compressible form of the conservation equations to allow for simulations of flight conditions. The scheme is capable of resolving the large scale differences involved. A turbulent base-flow was generated by mimicking an experimental setup. A JVG configuration was test by introducing a jet disturbance into the turbulent boundary layer flow and the effect on the boundary layer was evaluated. The simulated case does not show the development of longitudinal vortices but of streak structures and strong spanwise deflection of the mean flow. Further simulations are to be undertaken with increased spanwise jet nozzle distance.

## Acknowledgements

## References

[1] J. P. Johnston, M. Nishi: "Vortex Generator Jets – a Means for Flow Separation Control". AIAA Journal **28**, 1990, pp. 989-994.

[2] D. A. Compton, J. P. Johnston: "Streamwise Vortex Production by Pitched and Skewed Jets in a Turbulent Boundary Layer". AIAA Journal **30**, 1992, pp. 640-647.

[3] G. Godard, J. M. Foucaut, M. Stanislas: "Control of a decelerating boundary layer: Parts 1,2,3". Aerospace Science and Technology **10**, 2006.

[4] M. Casper, C. J. Kähler, R. Radespiel: "Fundamentals of Boundary Layer Control with Vortex Generator Jet Arrays". AIAA Flow Control Conference, 2008.

[5] S. K. Lele: "Compact Finite Difference Schemes with Spectral-like Resolution". J. Comp. Phys. **103**, 1992, pp. 16-42.

[6] M. J. Kloker: "A robust high-order split-type compact FD scheme for spatial direct numerical simulation of boundary-layer transition". Appl. Sci. Res. **59**, 1998, pp. 353-377.

[7] P. R. Spalart: "Direct simulation of a turbulent boundary layer up to $R_\theta = 1410$", J. Fluid Mech. **187**, 1988.

[8] J. Jeong, F. Hussain: "On the identification of a vortex", J. Fluid Mech. **285**, 1995, pp. 69-94.